AGU PUBLICATIONS

Geophysical Research Letters

RESEARCH LETTER
10.1002/2014GL060495

Key Points:
- Longer nonfrozen periods linked to summer greenness decline across NA
- Drought indicator and precipitation pattern confirm summer drought signal
- Seasonal shift in hydrology is a leading drought factor in northern ecosystems

Supporting Information:
- Readme
- Figures S1–S7

Correspondence to:
W. Buermann,
w.buermann@leeds.ac.uk

Citation:
Parida, B. R., and W. Buermann (2014), Increasing summer drying in North American ecosystems in response to longer nonfrozen periods, *Geophys. Res. Lett.*, *41*, 5476–5483, doi:10.1002/2014GL060495.

Received 9 MAY 2014
Accepted 16 JUL 2014
Accepted article online 18 JUL 2014
Published online 1 AUG 2014

Increasing summer drying in North American ecosystems in response to longer nonfrozen periods

Bikash R. Parida[1] and Wolfgang Buermann[2]

[1]Department of Civil Engineering, Shiv Nadar University, Dadri, India, [2]Institute for Climate and Atmospheric Science, School of Earth and Environment, University of Leeds, Leeds, UK

Abstract In snow-dominated northern ecosystems, spring warming is predicted to decrease water availability later in the season and recent findings suggest that corresponding negative impacts on plant productivity and wildfire frequency are already observable. Here we estimate the overall vulnerability of North American ecosystems to warming-related seasonal shifts in hydrology through identifying robust interannual linkages between nonfrozen periods, peak-to-late summer vegetation greenness, and an indicator of drought for 1982–2010. Our results show that longer nonfrozen periods earlier in the year are persistently associated with declines in peak-to-late summer greenness and moisture availability across large portions of North America. Hereby, vulnerabilities increase markedly across the dominant land covers with decreasing annual precipitation rates, lowering contributions of summer rainfall, and increasing altitude. The implications are that in a warmer world, seasonal hydrological shifts may emerge as a leading factor for summer drought in relatively dry temperate-forested ecosystems and across the northern high latitudes.

1. Introduction

Across North American (NA) temperate and high-latitude regions, rising temperatures over roughly the last five decades are characterized by a distinct seasonal pattern, with most of the warming being observed in winter and spring [*Karl et al*., 1996; *Bonsal et al*., 2001; *Cayan et al*., 2001; *Hengeveld et al*., 2005]. This spring warming has led to increases in the length of the nonfrozen period (inferred from temperature records) by approximately 2–4 d/decade since 1950 [*Easterling*, 2002; *Feng and Hu*, 2004]. A newly available long-term (1979–2010) freeze-thaw record based on satellite microwave measurements shows also a lengthening of the average nonfrozen period in NA by 3 d/decade which is largely driven by earlier spring thawing consistent with the seasonal temperature trends [*Kim et al*., 2012].

While generally a lengthening of the growing season across northern latitudes may be beneficial for vegetation productivity [*Xu et al*., 2013] and carbon sequestration [*Graven et al*., 2013], earlier spring onsets and snowmelt in conjunction with summer warming are thought to be the leading factors for a precipitous increase in wildfires in the western U.S. and Canada in the last three decades [*Stocks et al*., 2002; *Westerling et al*., 2006]. The earlier onset of spring alters seasonal hydrology and vegetation phenology pattern through early runoff, increased evapotranspiration, and increased snow sublimation [*Barnett et al*., 2005; *Jepsen et al*., 2012] with the combined effects leading to drier conditions around the midst of the growing season.

Recent findings suggest that this mechanism for summer drought operates very efficiently also across NA boreal forests, where over large portions consistent interannual covariations between earlier spring onset and reduced peak-to-late summer plant growth have been observed [*Buermann et al*., 2013]. However, the summer drought signal associated with an earlier spring onset has not been verified yet with soil moisture or drought indicators. Further, we also posit that this spring onset-summer drought mechanism may operate at continental scales across most of northern snow-dominated ecosystems rather than at regional scales or specific to a particular land cover, since many of northern ecosystems rely on winter snowpacks as an important source of water [*Barnett et al*., 2005].

In this study, we therefore examine the impact of longer nonfrozen periods during roughly the first half of the year on subsequent summer ecohydrological conditions across all of NA temperate and high-latitude nonmanaged ecosystems. Hereby, we exploit long-term (1982–2010) microwave and optical satellite records

to infer nonfrozen periods and vegetation greenness and also make use of an updated drought metric that is driven by climate input data (see section 2). A particular focus is to assess the vulnerability of specific land covers to summer drying associated with longer nonfrozen periods and how precipitation pattern (annual totals and seasonal distribution) and elevation modulate this vulnerability.

2. Data and Methods

For this study, we analyzed a diverse set of ground- and satellite-based gridded data that represent vegetation greenness and hydrological surface conditions for the study period 1982 to 2010. For satellite vegetation greenness, we obtained an improved and updated version (3g) of the advanced very high resolution radiometer-based bimonthly normalized difference vegetation index (NDVI) data at 8 km spatial resolution [*Pinzon and Tucker*, 2014]. NDVI is calculated from optical near-infrared and red surface reflectances and commonly used as a surrogate measurement of plant photosynthetic activity [*Myneni et al*., 1995]. Nonfrozen periods of the land surface were estimated from a daily freeze-thaw record based on measurements from the satellite scanning multichannel microwave radiometer (SMMR) and Special Sensor Microwave Imager (SSM/I) at 25 km spatial resolution [*Kim et al*., 2012]. The length of the nonfrozen period (NFP) during the roughly first half of the year was determined through counting the nonfrozen days from January to August (denoted as NFP_{JanAug}). This seasonality indicator captures also relatively short-term freezing events even after spring onset and thus may capture related effects on surface hydrology even better than the timing of spring onset. In addition, we also obtained monthly relatively high-resolution (0.5°) gridded precipitation and temperature fields from the Climatic Research Unit (CRU TS3.21) [*Harris et al*., 2013]. Further, land cover-specific investigations are based on the MOD12C1 land cover classification at 5 km spatial resolution [*Friedl et al*., 2002]. Since our focus is snow-dominated regions, we included in our analyses only vegetated nonmanaged NA ecosystems in the latitude band from 30°N to the northern limit (Figure S1 in the supporting information).

Last, for drought characterization we obtained monthly Palmer Drought Severity Index (PDSI) data at 0.5° spatial resolution [*Zhao and Running*, 2010]. Input data for the PDSI include precipitation data from the Global Historical Climatology Network [*Chen et al*., 2002], evaporation demand (National Centers for Environmental Prediction/Department of Energy II), and soil water holding capacity as a function of soil texture. A lower (higher) PDSI value is indicative of a drier (wetter) climate, respectively. It should be noted that this drought index does not account explicitly for the effects of seasonal changes in snow melt and runoff as well as vegetation activity [*Dai*, 2011] and thus may not fully capture the soil moisture status during the peak of the growing season. Given these caveats, we evaluated the consistency of the PDSI against an ensemble of soil moisture outputs from a set of more complex hydrological models that participated in the integrated project water and global change (WATCH) [*Weedon*, 2011]. Corresponding results show the widespread robust (positive) interannual covariations between summer soil moisture (from WATCH) and PDSI over our study region suggesting the PDSI provides a credible estimate of moisture status (Figure S2 in the supporting information). Furthermore, several studies have shown reasonably good agreement between the PDSI and observed stream flow as well as soil moisture during warm seasons [*Dai*, 2011].

All satellite (NDVI, land cover) and climate (e.g., PDSI) fields were aggregated (pixel aggregate)/downscaled (nearest neighbor) to a common 0.25° spatial grid on which all statistical analyses were performed. With a focus on identifying interannual linkages, original data were detrended prior to computing (Pearson's) grid point correlations. No single optimal solution for removing trends in these relatively short and often complex satellite and climate time series exists [*Zhou et al*., 2001]. We, therefore, used two different detrending methods for assessing the robustness of the interannual covariation patterns: (i) removal of linear trends (determined through least squares linear regression) over the entire study period 1982–2010 and (ii) first differences determined through changes in successive years. Student's *t* tests are used throughout to evaluate statistical significance of correlations.

3. Results

In the first step, we explored patterns in the interannual covariations between nonfrozen periods during the roughly first half of the year (NFP_{JanAug}) and subsequent peak-to-late summer NDVI for 1982–2010. Corresponding results document continental-scale negative correlation patterns over NA ecosystems (Figures 1a and 1c), implying that longer nonfrozen periods during the first half of the year are consistently

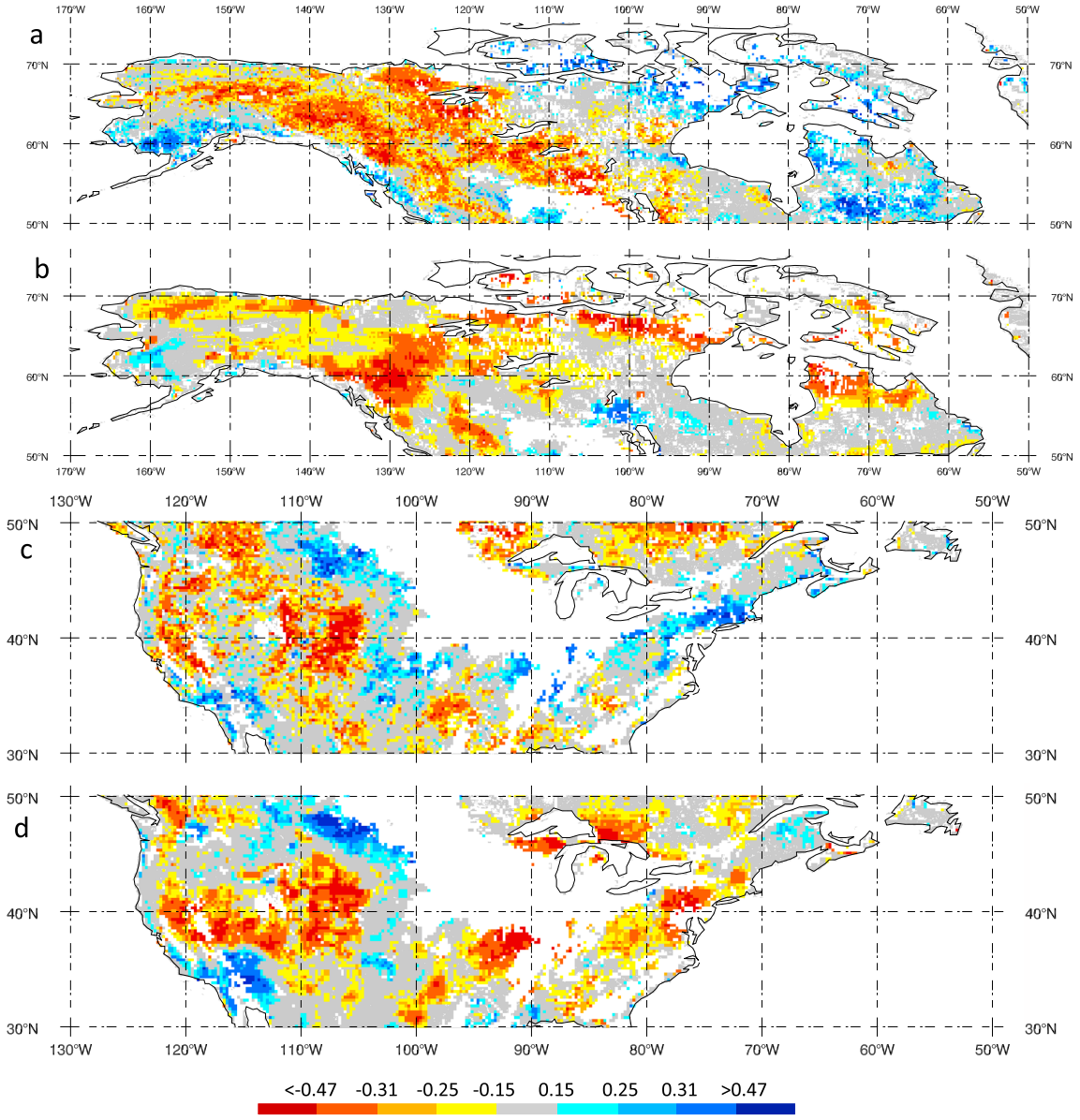

Figure 1. Interannual covariations between the length of nonfrozen period during the roughly first half of the year and subsequent summer greenness as well as drought. Maps show grid point correlations for the period 1982–2010 between the NFP_{JanAug} and peak-to-late summer (a, c) NDVI and (b, d) PDSI. For the northern high latitudes (Figures 1a and 1b) peak-to-late summer is defined as July through August, whereas for the temperate zones (Figures 1c and 1d) this epoch is defined as August through September. At each grid point, original data have been detrended via removal of linear trends for 1982–2010 prior to correlations. Absolute Pearson correlation values greater than 0.31 are statistically significant ($p < 0.1$).

associated with declines in peak-to-late summer vegetation greenness and vice versa. Increased vulnerabilities (more robust negative correlation patterns) are evident over the climatologically drier regions of western U.S. and the interior of Alaska as well as across western and interior Canada. In contrast, positive correlations (peak-to-late summer greenness benefits from longer nonfrozen epochs and vice versa) are spatially more confined in regions surrounding the Hudson Bay, the U.S. Great Plains as well as along the U.S. East coast and the northern portion of the NA West coast.

Our working hypothesis is that these observed relationships between longer nonfrozen periods in the first half of the year and decreased peak-to-late summer greenness can be explained by reduced soil moisture resulting from increased evapotranspiration and early runoff earlier in the growing season. To further and

independently test this assertion, we also analyzed interannual covariations between the NFP_{JanAug} and peak-to-late summer PDSI for 1982–2010. Results also show the widespread negative correlation patterns (Figures 1b and 1d) indicating that longer (shorter) nonfrozen periods during the first half of the year are consistently linked to peak-to-late summer water deficits (surpluses). These negative patterns are broadly colocated with those based on the covariations between the NFP_{JanAug} period and peak-to-late summer NDVI (Figures 1a and 1c). Further, across these coinciding patterns the PDSI and NDVI fields during peak-to-late summer show also strong positive interannual covariations (Figure S3 in the supporting information) in line with the notion that the PDSI does capture the soil moisture status in this season to some extent, which in turn exerts a strong climatic constraint on plant growth. In contrast and as one may expect, over the climatologically wetter more eastern NA regions where peak-to-late summer greenness benefits from longer nonfrozen periods earlier in the year (Figures 1a and 1c), the PDSI does not serve as a robust predictor of interannual NDVI variability during peak-to-late summer (Figure S3 in the supporting information).

A noteworthy and exceptional pattern emerges over portions of the U.S. Great Plains (~100°–110°W and 45°–50°N). Over these relatively dry (total annual rainfall ~300 mm; Figure S4 in the supporting information) vast grassland regions, the PDSI appears to be a reliable predictor of interannual variations in NDVI during peak-to-late summer (Figure S3 in the supporting information), and the year-to-year covariations of these two variables with the length of nonfrozen periods in the first half of the year are also both positive and spatially colocated (Figures 1c and 1d). Further analyses over these regions (not shown) show that longer nonfrozen periods in the early to middle growing season are associated with increased summer rainfall and, hence, increased PDSI as well as NDVI (giving rise to the observed positive correlation between NFP_{JanAug} and NDVI as well as PDSI, respectively). These peculiar links may be related to increased water cycling in years with longer nonfrozen periods early in the year over the U.S. Great Plains, a region which is known for their strong coupling between soil moisture and precipitation [*Koster et al*., 2004].

The robustness of these spatial correlation patterns with a focus on interannual timescales was assessed by repeating the analysis with an alternative method for removing trends in the original data (see section 2). Results show that the patterns are generally robust against method (Figure 1 and Figure S5 in the supporting information), except for NFP_{JanAug}-PDSI correlations in the northern high latitudes where some deviations can be observed. However, across these more northern regions the PDSI is also known to be a less reliable drought indicator, since processes that may be more important such as frozen soil, snow accumulation, and melt are not considered [*Heim*, 2002; *Dai et al*., 2004].

In a next step, we explored the vulnerability of specific NA land covers to this "summer drought mechanism" and how the annual total rainfall rates and seasonal distributions influence this vulnerability. Within the NA boreal zone (>50°N), dominant land covers with relatively large vulnerable areal proportions (Figures 2a–2d), include evergreen needleleaf forests (~20–24% areal proportions), mixed forests (~22–27%), and woody savannas (~29–31%). Northern open shrublands (also known as tundra) show a lower vulnerable areal proportion (~10%), but equal evergreen needleleaf forests in terms of total vulnerable area because of their vast geographic distribution (Figures 2a and 2c). Within the temperate regions, the most vulnerable land covers in regard to both areal proportions and total vulnerable area (Figures 2e–2h) are evergreen needleleaf forests (~27–31% areal proportions) and grasslands (~14–18%). Mixed forests (~7–12%) and open shrublands (~9–17%) showing a somewhat lower vulnerability.

Scatterplots of summer (JJA) rainfall proportions against the annual total precipitation show that across most of the vulnerable regions within the dominant NA land covers higher clustering occurs when the annual total precipitation is typically below 500 mm and when the proportion of summer precipitation to total annual rainfall is below 50% (Figure 2 and Figure S4 in the supporting information). In cases where these summer rainfall proportions are comparably low (~25%), vulnerability for single land covers is also prevalent even in relatively wet regions (e.g., boreal and temperate needleleaf forests as well as temperate mixed forests and grasslands). At the other extreme, most boreal land covers in relatively dry regions (annual total rainfall >250 mm) show high vulnerability despite receiving most of their annual rainfall in the summer months.

In the final step, we explored the influence of elevation on the efficacy of the summer drought mechanism with linkage to longer nonfrozen periods, since soil storage capacities may be influenced by topographic

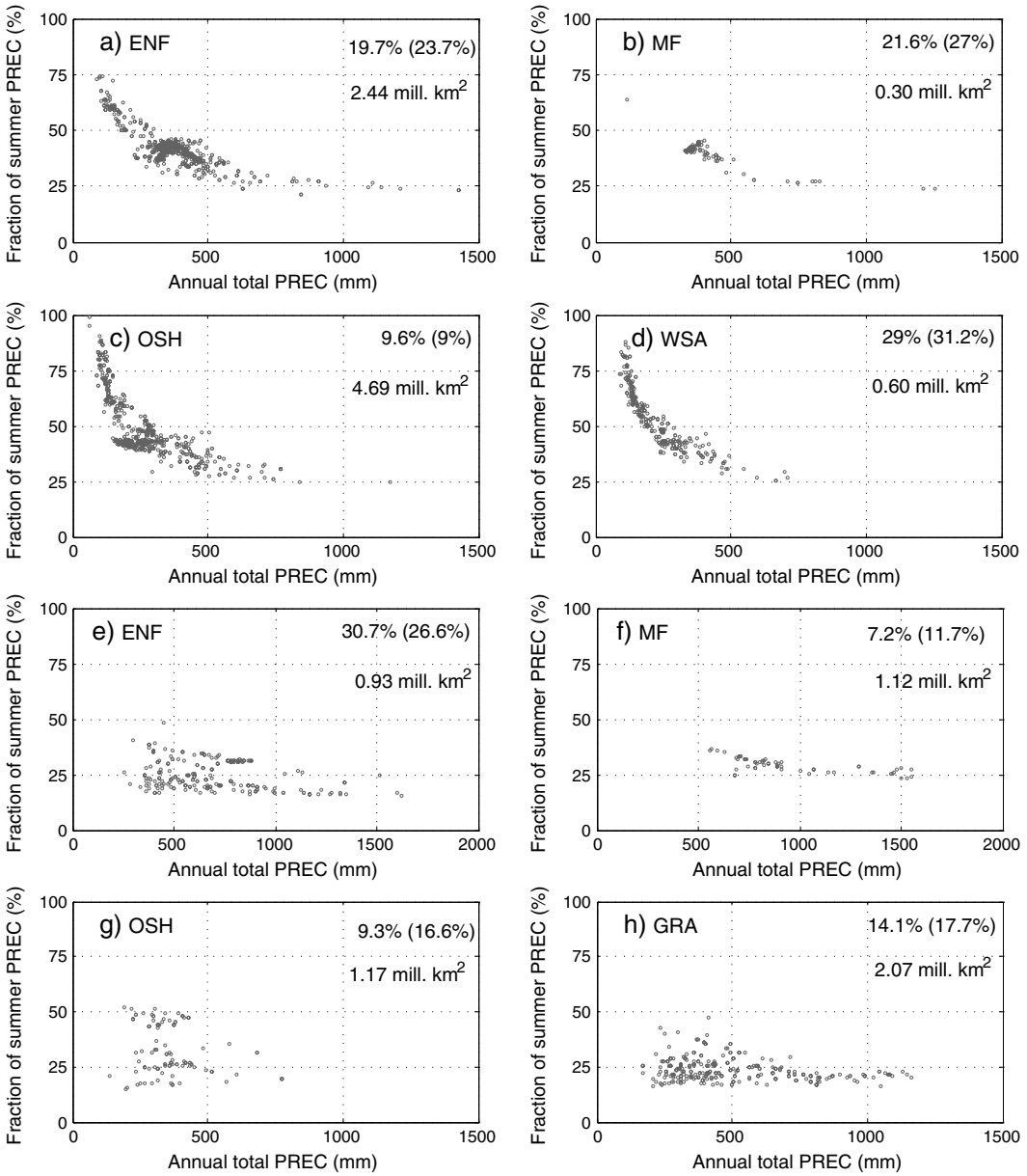

Figure 2. Land cover and precipitation influence on vulnerability to summer drying linked to longer nonfrozen periods. For each dominant land cover (Figure S1), panels depict scatterplots of the annual total precipitation (PREC) versus ratio of summer (June-July-August (JJA)) precipitation over the annual total precipitation, based on the climatology for the period 1982–2010. (a–d) NA boreal land covers (50°N–75°N); and (e–h) temperate land covers (30°N–50°N). For each land cover, total area and two estimates of vulnerable areal proportions (%) are also provided in the insets. Here vulnerable areas are defined as those that exhibit significant ($p < 0.1$) negative interannual covariations between the NFP_{JanAug} and peak-to-late summer NDVI (see Figures 1a and 1c, and Figures S5a and S5c in the supporting information). The two estimates of vulnerable areal proportions are based on two methods of removing trends in the original data prior correlations analyses (see section 2; values in brackets are based on the first differences method). Land covers are abbreviated as evergreen needleleaf forest (ENF), mixed forests (MF), open shrublands (OSH), woody savannas (WSA), and grasslands (GRA). Corresponding results for deciduous broadleaf forests (DBF) and WSA in the temperate zones are not shown since either vulnerable areal proportions (1–6% for DBF) or total vulnerable area are less extensive (0.03–0.06 million km^2 for WSA).

variations [*Garcia and Tague*, 2014]. The results show that vulnerable areal proportions as a function of altitude reflect unimodal distributions for most dominant NA boreal land covers, but corresponding peak vulnerabilities depend on land cover (Figure 3a). For example, evergreen needleleaf forests appear more vulnerable at altitudinal ranges between 600 and 900 m, whereas for woody savannas (900–1200 m) and

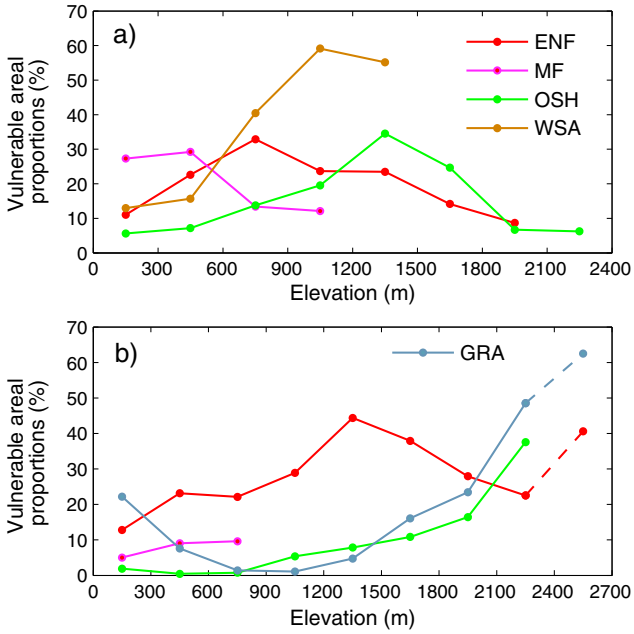

Figure 3. Elevational influence on vulnerability to summer drying linked to longer nonfrozen periods. Panels display vulnerable areal proportions, defined as in Figure 2, for successive 300 m elevational intervals and dominant NA land covers, located in the (a) boreal (50°N–75°N) and (b) temperate (30°N–50°N) zones, respectively.

open shrublands (1200–1500 m), these levels are shifted toward higher elevations. Across vulnerable temperate land covers, only evergreen needleleaf forests show a similar elevational dependency as observed in the boreal zones, but peak vulnerability levels at these lower latitudes are markedly shifted toward higher elevations (~1200–1500 m). For grasslands and open shrublands, the efficiency of the drought mechanism increases gradually at altitudes above ~1200 m and more sharply at relatively high altitudes (>2100 m). Corresponding results for very high elevations (>2400 m) should be interpreted with caution since the areal extent of land covers at these altitudes is very small and both the satellite optical (used to infer vegetation greenness) and microwave (for nonfrozen periods) data are less reliable because of topographic shading effects in very high mountain regions [e.g., *Kim et al.*, 2012].

4. Discussion and Conclusion

The overall good agreement in the spatial patterns pertaining to the interannual covariations between longer nonfrozen periods during roughly the first half of the year and reduced peak-to-late summer vegetation greenness as well as water availability may serve as the first line of hydrologic evidence that these joint large-scale linkages are associated with a summer drought phenomena. This key finding is even more intriguing since the exploited drought indicator may underestimate the true soil moisture status in summer substantially as it does not encapsulate information on seasonal changes in snow melt, runoff, vegetation phenology, and root development [*Dai et al.*, 2004]. In line with these results, a few field-based studies (based on eddy covariance flux towers) have reported declines in annual net ecosystem productivity owing to temporal shifts to earlier spring onsets and snow melt that led to increases in early season runoff and evapotranspiration and decreasing water availability in the later part of the growing season [*Welp et al.*, 2007; *Sacks et al.*, 2007; *Hu et al.*, 2010].

Our results also suggest that forested ecosystems, including temperate and boreal evergreen needleleaf forests as well as boreal mixed forests and woody savannas located predominantly in the western climatologically drier portion of NA, represent the land covers that are more vulnerable to this summer drought mechanism. However, corresponding vulnerabilities are also widespread among more open ecosystems including temperate grasslands and northern tundra. Within these land covers, annual amount and seasonal distribution of rainfall rates are strong determinants of vulnerability. We find that vulnerability increases with lower annual total rainfall and lower proportions of summer rainfall as perhaps anticipated since these relations indicate overall drought vulnerability and a greater reliance on winter snow packs as a source of water [*Barnett et al.*, 2005]. In fact, the existence of such dependencies provides another independent hydrologic-based evidence for this summer drought mechanism with links to longer nonfrozen periods earlier in the year.

One may hypothesize that variations in summer rainfall have a greater influence on peak-to-late summer greenness and moisture status than those associated with nonfrozen period variability during roughly the first half of the year. A corresponding supplementary analysis shows that the (positive) influence of summer rainfall on peak-to-late summer greenness status is particularly strong across the temperate grasslands and open shrublands (Figure S6 in the supporting information). Over the northern high latitudes and temperate more forested ecosystems, however, the influence of summer rainfall is substantially weaker (and even its

direction shifts from positive to negative) and is comparable to the one linked to early to middle season nonfrozen periods (Figure 1 and Figure S6 in the supporting information). These perhaps not anticipated results could be explained by a number of factors, one being related to the adverse influence of cloud cover (that accompanies rainfall) on plant growth, a known colimiting factor in these regions [*Nemani et al*., 2003]. Another potential factor is the observation that over the northern high latitudes, the often abundant summer rainfall (but also note that the NA high latitudes are climatologically relatively dry areas; see Figure S4 in the supporting information) does aid in replenishing soil moisture near the surface but may be less effective in recharging deeper soil layers (where trees generally have their roots) because a large fraction is lost to (re) evaporation [*Barichivich et al*., 2014]. Summer rainfall exclusion experiments conducted in interior Alaska also show that tree growth in well-drained upland forests is sustained primarily by snowmelt water and is not substantially affected by summer rainfall deficits [*Yarie*, 2008].

Further, our results also show that elevation has a significant influence on the vulnerability of the dominant NA land covers to this summer drought mechanism, consistent with earlier findings at more regional scales [*Westerling et al*., 2006]. The general pattern is that vulnerability increases with increasing altitudes up to a certain level, whereby for temperate latitudes, regions of peak vulnerability stretch over substantially higher elevational ranges. These results are broadly consistent with reduced soil storage capacities due steeper slopes and well-drained surfaces at higher elevations [*Garcia and Tague*, 2014], whereas at very high elevations (especially in the boreal zone), low temperature constrains on plant growth may become a more dominant factor.

In an annual sense, vegetation growth in snow-dominated northern ecosystems is generally considered temperature and radiation limited [*Nemani et al*., 2003]. As a result, rapid warming in northern mid- and high-latitudes throughout the last several decades appear to have led to longer growing seasons, increased photosynthetic activity and carbon sequestration [*Randerson et al*., 1999; *Tanja et al*., 2003; *Richardson et al*., 2010; *Xu et al*., 2013; *Graven et al*., 2013]. Our results show that summer drying and reduced photosynthetic activity in response to longer nonfrozen periods earlier in the year can be robustly detected in observations covering the last three decades. Because this summer drought mechanism acts at continental scales, it is not unlikely that this factor has substantially modulated the general response of northern ecosystems to recent warming trends.

Increasing heat and drought stress on the world's forests is presently emerging as global scale phenomena [*Allen et al*., 2010], and these factors are also key in responses of ecosystems under future climate projections [*Sitch et al*., 2008; *Williams et al*., 2013]. In this regard, the significance of summer drying with linkages to longer nonfrozen periods specifically in the early to middle growing season across northern ecosystems remains an open question. On one hand, there appears to be a direct link between spring warming, associated longer nonfrozen periods (Figure S7 in the supporting information) and summer drying. One the other hand, this drought mechanism acts specifically toward reducing peak-to-late summer plant growth and some ecosystems may be more resilient to such relative short episodes of drought. Arguably the largest impact will be on high-altitude needleleaf-dominated forests in climatologically relative dry temperate and boreal zones where increasing peak-to-late summer drying may influence important disturbance regimes (e.g., fires and insects) which in turn may lead to rapid declines in forest extent.

In respect to carbon sequestration, northern forested ecosystems are credited as a sustained land-based carbon sink for the contemporary period (1990–2007) [*Pan et al*., 2011]. However, longer nonfrozen periods owing largely to warmer springs may pose an additional constraint on the future carbon sink in conjunction with projected declines in summer precipitation over midlatitude regions of the Northern Hemisphere [*Rowell*, 2009; *Christensen et al*., 2013]. The influence of this "longer nonfrozen period and summer drought" mechanism on the carbon balance of northern ecosystems needs further study with coupled climate-carbon cycle models.

Acknowledgments
This research is funded by a grant from the National Aeronautics and Space Administration Carbon Cycle Science Program (grant NNX11AD45G). We are indebted to John Kimball group for providing updated freeze/thaw record from the SMMR and SSM/I sensors. We thank Shiv Nadar University, India, for providing computing facilities.

The Editor thanks two anonymous reviewers for their assistance in evaluating this paper.

References

Allen, C. D., et al. (2010), A global overview of drought and heat-induced tree mortality reveals emerging climate change risks for forests, *For. Ecol. Manage.*, *259*, 660–84.

Barichivich, J., K. R. Briffa, R. Myneni, G. van der Schrier, W. Dorigo, C. J. Tucker, T. J. Osborn, and T. M. Melvin (2014), Temperature and snow-mediated moisture controls of summer photosynthetic activity in northern terrestrial ecosystems between 1982 and 2011, *Remote Sens.*, *6*, 1390–1431.

Barnett, T. P., J. C. Adam, and D. P. Lettenmaier (2005), Potential impacts of a warming climate on water availability in snow-dominated regions, *Nature*, *438*, 303–309, doi:10.1038/nature04141.

Bonsal, B. R., X. Zhang, L. A. Vincent, and W. D. Hogg (2001), Characteristics of daily and extreme temperatures over Canada, *J. Clim.*, *14*, 1959–1976.

Buermann, W., P. R. Bikash, M. Jung, D. H. Burn, and M. Reichstein (2013), Earlier springs decrease peak summer productivity in North American boreal forests, *Environ. Res. Lett.*, *8*, 024027, doi:10.1088/1748-9326/8/2/024027.

Cayan, D. R., S. A. Kammerdiener, M. D. Dettinger, J. M. Caprio, and D. H. Peterson (2001), Changes in the onset of spring in the western United States, *Bull. Am. Meteorol. Soc.*, *82*, 399–416.

Chen, M., P. Xie, J. E. Janowiak, and P. A. Arkin (2002), Global land precipitation: A 50-yr monthly analysis based on gauge observations, *J. Hydrometeorol.*, *3*, 249–266.

Christensen, J. H., et al. (2013), Climate phenomena and their relevance for future regional climate change, in *Climate Change 2013: The Physical Science Basis. Contribution of Working Group I to the Fifth Assessment Report of the Intergovernmental Panel on Climate Change*, chap. 14, edited by T. F. Stocker et al., pp. 1217–1308, Cambridge Univ. Press, New York.

Dai, A. (2011), Characteristics and trends in various forms of the Palmer Drought Severity Index during 1900–2008, *J. Geophys. Res.*, *116*, D12115, doi:10.1029/2010JD015541.

Dai, A., K. E. Trenberth, and T. Qian (2004), A global dataset of Palmer Drought Severity Index for 1870–2002: Relationship with soil moisture and effects of surface warming, *J. Hydrometeorol.*, *5*, 1117–1130.

Easterling, D. R. (2002), Recent changes in frost days and the frost-free season in the United States, *Bull. Am. Meteorol. Soc.*, *83*, 1327–1332.

Feng, S., and Q. Hu (2004), Changes in agro-meteorological indicators in the contiguous United States: 1951–2000, *Theor. Appl. Climatol.*, *78*, 247–264.

Friedl, M., et al. (2002), Global land cover mapping from MODIS: Algorithms and early results, *Remote Sens. Environ.*, *83*, 287–302.

Garcia, E. S., and C. L. Tague (2014), Climate regime and soil storage capacity interact to effect evapotranspiration in western United States mountain catchments, *Hydrol. Earth Syst. Sci. Discuss.*, *11*, 2277–2319.

Graven, H. D., et al. (2013), Enhanced seasonal exchange of CO_2 by northern ecosystems since 1960, *Science*, *341*, 1085–1089.

Harris, I., P. Jones, T. Osborn, and D. Lister (2013), Updated high-resolution grids of monthly climate observations—The CRU TS3.10 dataset, *Int. J. Climatol.*, 623–642, doi:10.1002/joc.3711.

Heim, R. R., Jr. (2002), A review of twentieth-century drought indices used in the United States, *Bull. Am. Meteorol. Soc.*, *83*, 1149–1165.

Hengeveld, H., B. Whitewood, and A. Fergusson (2005), *An Introduction to Climate Change: A Canadian Perspective*, 55 pp., Environment Canada, Downsview, Ontario.

Hu, J., D. J. P. Moore, S. P. Burns, and R. K. Monson (2010), Longer growing seasons lead to less carbon sequestration by a subalpine forest, *Global Change Biol.*, *16*, 771–783.

Jepsen, S. M., N. P. Molotch, M. W. Williams, K. E. Rittger, and J. O. Sickman (2012), Interannual variability of snowmelt in the Sierra Nevada and Rocky Mountains, United States: Examples from two alpine watersheds, *Water Resour. Res.*, *48*, W02529, doi:10.1029/2011WR011006.

Karl, T., R. Knight, D. Easterling, and R. Quayle (1996), Indices of climate change for the United States, *Bull. Am. Meteorol. Soc.*, *77*, 279–292.

Kim, Y., J. S. Kimball, K. Zhang, and K. C. McDonald (2012), Satellite detection of increasing Northern Hemisphere non-frozen seasons from 1979 to 2008: Implications for regional vegetation growth, *Remote Sens. Environ.*, *121*, 472–487.

Koster, R. D., et al. (2004), Regions of strong coupling between soil moisture and precipitation, *Science*, *305*, 1138–1140.

Myneni, R. B., F. G. Hall, P. J. Sellers, and A. L. Marshak (1995), The meaning of spectral vegetation indices, *IEEE Trans. Geosci. Remote Sens.*, *33*, 481–486.

Nemani, R. R., C. D. Keeling, H. Hashimoto, W. M. Jolly, S. C. Piper, C. J. Tucker, R. B. Myneni, and S. W. Running (2003), Climate-driven increases in global terrestrial net primary production from 1982 to 1999, *Science*, *300*, 1560–1563.

Pan, Y., et al. (2011), A large and persistent carbon sink in the world's forests, *Science*, *333*(6045), 988–993, doi:10.1126/science.1201609.

Pinzon, J. E., and C. J. Tucker (2014), A non-stationary 1981–2012 AVHRR NDVI3g time series, *Remote Sens.*, *6*(8), 6929–6960.

Randerson, J. T., C. B. Field, I. Y. Fung, and P. P. Tans (1999), Increases in early season ecosystem uptake explain recent changes in the seasonal cycle of atmospheric CO_2 at high northern latitudes, *Geophys. Res. Lett.*, *26*, 2765–2768, doi:10.1029/1999GL900500.

Richardson, A. D., et al. (2010), Influence of spring and autumn phonological transitions on forest ecosystem productivity, *Philos. Trans. R. Soc. B*, *365*, 3227–3246, doi:10.1098/rstb.2010.0102.

Rowell, D. P. (2009), Projected midlatitude continental summer drying: North America versus Europe, *J. Clim.*, *22*, 2813–2833.

Sacks, W. J., D. S. Schimel, and R. K. Monson (2007), Coupling between carbon cycling and climate in a high-elevation, subalpine forest: A model-data fusion analysis, *Oecologia*, *4*, 54–68.

Sitch, S., et al. (2008), Evaluation of the terrestrial carbon cycle, future plant geography and climate-carbon cycle feedbacks using five Dynamic Global Vegetation Models (DGVMs), *Global Change Biol.*, *14*, 1–25.

Stocks, B. J., et al. (2002), Large forest fires in Canada, 1959–1997, *J. Geophys. Res.*, *107*(D1), 8149, doi:10.1029/2001JD000484.

Tanja, S., et al. (2003), Air temperature triggers the recovery of evergreen boreal forest photosynthesis in spring, *Global Change Biol.*, *9*, 1410–1426, doi:10.1046/j.1365-2486.2003.00597.x.

Weedon, G. P. (2011), Creation of the WATCH 20th century ensemble product, WATCH Technical Report Number 37, UK Met Office.

Welp, L. R., J. T. Randerson, and H. P. Liu (2007), The sensitivity of carbon fluxes to spring warming and summer drought depends on plant functional type in boreal forest ecosystems, *Agric. For. Meteorol.*, *147*, 172–85.

Westerling, A. L., H. G. Hidalgo, D. R. Cayan, and T. W. Swetnam (2006), Warming and earlier spring increase western U.S. forest wildfire activity, *Science*, *313*, 940–943.

Williams, A. P., et al. (2013), Temperature as a potent driver of regional forest drought stress and tree mortality, *Nat. Clim. Change*, *3*(3), 292–297.

Xu, L., et al. (2013), Temperature and vegetation seasonality diminishment over northern lands, *Nat. Clim. Change*, *3*, 581–586.

Yarie, J. (2008), Effects of moisture limitation on tree growth in upland and floodplain forest ecosystems in interior Alaska, *For. Ecol. Manage.*, *256*, 1055–1063.

Zhao, M., and S. W. Running (2010), Drought-induced reduction in global terrestrial net primary production from 2000 through 2009, *Science*, *329*(5994), 940–943.

Zhou, L. M., C. J. Tucker, R. K. Kaufmann, D. Slayback, N. V. Shabanov, and R. B. Myneni (2001), Variations in northern vegetation activity inferred from satellite data of vegetation index during 1981 to 1999, *J. Geophys. Res.*, *106*, 20,069–20,083, doi:10.1029/2000JD000115.